

Anilino-dialkoxyquinazolines: Screening Epidermal Growth Factor Receptor Tyrosine Kinase Inhibitors for Potential Tumor Imaging Probes

Henry F. VanBrocklin^{1,*}, John K. Lim^{1,2}, Stephanie L. Coffing^{3,5}, Darren L. Hom¹, Kitaw Negash^{1,4}, Michele Y. Ono¹, Jennifer L. Gilmore³, Ianthe Bryant³, and David J. Riese II³

¹ Department of Functional Imaging, Lawrence Berkeley National Laboratory, Berkeley, CA 94720-8119

² Department of Radiology, University of California, San Francisco, CA 94143

³ Department of Medicinal Chemistry and Molecular Pharmacology, Purdue University, 1333 Heine Pharmacy Building, West Lafayette, IN 47907

² Current Address: Hitachi High Technologies America, Inc., San Jose, CA 95134

⁴ Current Address: American Cyanamide Co., Agricultural Research Division, Princeton, NJ 08543

⁵ Current Address: Pfizer Central Research, Groton, CT 06349

*Corresponding Author:
Henry F. VanBrocklin, Ph.D.
Lawrence Berkeley National Laboratory
1 Cyclotron Rd. MS55R0121
Berkeley, CA 94720-8119
Phone: 510.486.4083
Fax: 510.486.4768
E-mail: hfvanbrocklin@lbl.gov

Working Title: EGFR Inhibitors as Imaging Probes

Abstract

The epidermal growth factor receptor (EGFR), a long-standing drug development target, is also a desirable target for imaging. Sixteen dialkoxyquinazoline analogs, suitable for labeling with positron-emitting isotopes, have been synthesized and evaluated in a battery of *in vitro* assays to ascertain their chemical and biological properties. These characteristics provided the basis for the adoption of a selection schema to identify lead molecules for labeling and *in vivo* evaluation. A new EGFR tyrosine kinase radiometric binding assay revealed that all of the compounds possessed suitable affinity ($IC_{50} = 0.4 - 51$ nM) for the EGFR tyrosine kinase. All of the analogs inhibited ligand-induced EGFR tyrosine phosphorylation ($IC_{50} = 0.8 - 20$ nM). The HPLC-estimated octanol/ water partition coefficients ranged from 2.0-5.5. Four compounds, 4-(2'-fluoroanilino)- and 4-(3'-fluoroanilino)-6,7-diethoxyquinazoline as well as 4-(3'-chloroanilino)- and 4-(3'-bromoanilino)-6,7-dimethoxyquinazoline, possess the best combination of characteristics that warrant radioisotope labeling and further evaluation in tumor-bearing mice.

Introduction

Protein tyrosine kinases (PTKs), enzymes that phosphorylate tyrosine residues on functional proteins, are common mediators of signals that regulate many cellular processes. PTKs can be divided into two subgroups based on their structural characteristics, nonreceptor cytoplasmic PTKs and receptor tyrosine kinases (RTKs).¹ To date at least 20 families of receptor tyrosine kinases that share structural, most notably an intrinsic tyrosine kinase domain, and functional similarities have been classified.^{2,3} The epidermal growth factor receptor (EGFR) was one of the first oncogenes and receptor tyrosine kinases to be discovered.^{4,5} EGFR belongs to the ErbB family of receptors, which also includes ErbB2 (HER2/Neu), ErbB3 and ErbB4. These receptors are overexpressed in a variety of tumors.

EGFR tyrosine kinase phosphorylation is stimulated by epidermal growth factor (EGF) or transforming growth factor α (TGF α) binding to the extracellular ligand binding domain of the EGFR and subsequent receptor dimerization. Signal transduction initiated by these events regulates cellular proliferation, differentiation, motility, adhesion and apoptosis. These signaling processes play an important role in normal epithelial and stromal cell morphology; moreover, overexpression or aberrant signaling from EGFR and the other ErbB receptor family members has been shown to be a key determinant in tumor growth and proliferation.^{6,7}

Overexpression of EGFR has been found in head and neck tumors, gliomas, non-small cell lung carcinoma and tumors of the breast, ovaries, cervix, esophagus, bladder, prostate, and kidney.⁷ There is extensive literature on the clinical significance of increased EGFR expression and signaling in tumors and the relationship to other prognostic factors.^{8,9} In a majority of tumors poor survival rates correlate with EGFR overexpression. For example, EGFR overexpression has been detected in nearly 45 percent of the breast tumors studied¹⁰ and receptor overexpression is inversely correlated with patient survival.⁹ EGFR overexpression is also inversely correlated with estrogen receptor status, consistent with the failure of EGFR positive patients to respond to hormonal therapies.^{11,12} The relevance of EGFR expression in tumors to prognostic outcome supports the years of investment towards finding an EGFR-targeted therapeutic¹³⁻¹⁸ and the need for a diagnostic imaging agent. Development of an imaging agent might also be a valuable tool in the search for and the characterization of EGFR-targeted therapeutics.

Two potential targets for EGFR-based probes are the extracellular domain or the intracellular tyrosine kinase domain. Radioactive probes that bind to the extracellular domain of EGFR have been generated. EGF, the 53 amino acid, 6 kDa, natural ligand, binds to the EGFR with a K_d of 0.1-1.0 nM¹⁹ and has been labeled directly with iodine-123, iodine-125 and iodine-131. *In vitro* studies using [¹³¹I]EGF demonstrated its cytotoxic potential.²⁰ ¹²³I-EGF has been used to image cervical cancer in humans.²¹ In spite of its ability to localize in EGFR rich tissue, radioiodinated EGF rapidly degrades *in vivo* releasing radioiodine thereby reducing the lifetime of the label in the tumor.²² Iodinated dextran-EGF conjugates increase retention of the iodine by tumor cells but at the cost of higher molecular weight that affects tracer distribution.²⁰ EGF has been labeled with technetium-99m using a MAG3 or 2-iminothiolane chelate and was found to accumulate in tumor xenografts with more rapid clearance than labeled monoclonal antibodies (Mabs).²³⁻²⁵ Bifunctional chelation of indium-111 to EGF using diethylenetriaminepentaacetic acid (DTPA) has been shown to have cytotoxic effects *in vitro* and is being investigated as a potential radiotherapeutic agent.^{26,27} The imaging potential of ¹¹¹In-EGF was found to be inferior to a labeled anti-EGFR antibody, ¹¹¹In-DTPA-MAb 528 in tumor bearing rats.²⁸

Several MAb against EGFR have been developed as anti-tumor agents. The radioiodinated MAb, EGFR1, with high affinity for the EGFR has demonstrated good uptake in MCF-7 tumors grown in nude athymic mice²⁹ and good localization in human brain gliomas.³⁰ Likewise, the indium-111 labeled C225 MAb has been tested in patients with squamous cell lung carcinoma.³¹ A direct-labeled technetium-99m anti-EGFR antibody, ior egfr/r3, has demonstrated imaging sensitivity (84%), specificity (100%) and accuracy (86.5%) in human epithelial tumors.³² However, MAbs labeled with short-lived PET isotopes, in general, have demonstrated limited targeting success in large part due to pharmacokinetic constraints related mostly to their size.

To date no small organic molecules with affinity for the extracellular domain of the EGFR have been identified; however, a number of small molecules have been shown to be potent (nM to pM) inhibitors of the intracellular EGFR tyrosine kinase at the ATP binding site. A sampling of the different compound classes that inhibit EGFR phosphorylation is shown in Figure 1. The dialkoxy-

anilinoquinazolines (Figure 1) were chosen as the lead compounds in the present study based on the strong structure-activity data.³³⁻³⁵

The development of imaging agents based on the small molecule EGFR inhibitors has been a recent area of active research. A number of radiolabeled anilinoquinazoline analogs have been reported. The compounds incorporate labeled substituents on the A or C rings (see Figure 1) of the anilino- or benzylamino- quinazoline. The C ring substituted analogs include 4-(3'-[¹²⁵I]iodoanilino)^{36,37}, 4-(3'-[¹⁸F]fluoro-5'-trifluoromethylanilino)-³⁸, 4-(3',4'-dichloro-6'-[¹⁸F]fluoroanilino)-³⁸, and 4-(3'-chloro-4'-[¹⁸F]fluoroanilino)-³⁹. The 7-[¹⁸F]fluoroethoxy-⁴⁰ and the 6- or 7-[¹¹C]methoxy-^{40,41} constitute the A ring labeled analogs. Preliminary *in vitro* studies with the 3'-[¹²⁵I]iodo analog demonstrated receptor mediated uptake in cells containing high EGFR titer.³⁷ A study of the carbon-11 methoxy derivative demonstrated some uptake in human neuroblastoma xenografts in mice^{42,43}; however, the 20 min half-life of the carbon-11 may not allow adequate time for the development of good signal relative to background. Bonasera and colleagues evaluated five fluorine-18 labeled compounds.³⁸ They studied the 4-(4'-[¹⁸F]fluoroanilino)-dimethoxyquinazoline and the 4-(3',4'-dichloro-6'-[¹⁸F]fluoroanilino)-dimethoxyquinazoline in tumor-bearing mice. These tracers did not accumulate in the tumors nor was receptor-mediated uptake, based on blocking studies, observed for the latter probe. Low receptor affinity, high non-specific binding and probe metabolism may have contributed to the inability of these compounds to accumulate in tumor cells that overexpress EGFR.

Successful development of an imaging probe targeting a new biomarker, in this case EGFR, requires an adequate screening strategy for the selection of ligands to be carried forward for labeling and, ultimately, *in vivo* studies. It is neither economically nor logistically feasible to label and evaluate every compound in animal models. Likewise, navigating the structure activity relationships in the medicinal chemistry literature can be challenging with respect to choosing an appropriate imaging lead compound. For example, the fact that a small molecule is a potent EGFR inhibitor does not necessarily guarantee that it will possess desirable EGFR imaging characteristics such as high receptor affinity, high receptor selectivity, low non-specific binding, rapid clearance and suitable metabolism.

In the current study, a small series of dialkoxyquinazoline EGFR inhibitors suitable for labeling with fluorine-18 (110 min half-life positron-emitter) or carbon-11 (20 min half-life positron-emitter) has been synthesized. Appropriate assays have been developed to determine both functional and imaging characteristics, including a new radiometric binding assay to measure the affinity of the inhibitors for the enzyme. These studies provide the basis needed for the selection of ligands to be labeled and further evaluated as potential imaging agents for the non-invasive determination of EGF receptor density.

Results

Chemistry.

A small library of anilino- and benzyl-dialkoxyquinazoline compounds **10-17** were prepared by coupling 4-chloro-dialkoxyquinazoline **8** or **9** with the appropriate substituted aniline or benzylamine (Scheme 3). The 4-chloro-6,7-dimethoxyquinazoline was synthesized as previously reported from the 4,5-dimethoxyanthranilic acid **5**.³³ As the 4-(3'-bromoanilino)-6,7-diethoxyquinazoline was reported³³ to possess more potent biological activity than the corresponding 6,7-dimethoxy analog, we were interested in finding a convergent synthetic route suitable for the preparation of several diethoxy analogs. The previously reported two step conversion of the dimethoxy-bromoanilinoquinazoline **11c** to the diethoxy analog **10c** (Scheme 3), using a pyridinium hydrochloride melt to give the bishydroxy intermediate followed by O-alkylation with iodoethane, proceeded in a low 5.5% yield.³³ This was inadequate for the preparation of a series of the diethoxy analogs. Thus, we produced the 4,5-diethoxyanthranilic acid **4** by two methods (Scheme 1). Initially, a small amount of methyl 2-amino-4,5-diethoxybenzoate **3** was commercially available from Aldrich Specialty Chemical. The benzoate **3** was directly converted to **4** by saponification of the methyl ester. Alternatively, when the commercial supply was depleted, 4,5-diethoxybenzoic acid **1** was nitrated to give **2** followed by reduction of the nitro group to form the desired amino-benzoic acid **4** in moderate overall yield.

Preparation of the 4-chloroquinazolines followed a previously described procedure (Scheme 2).³³ Cyclization of the dialkoxyanthranilic acids, **4** or **5**, with formamidine hydrochloride at 210°C gave the corresponding dialkoxyquinazolinones, **6** or **7**, in 55-65% yield. The quinazolinones were subsequently

refluxed with oxalyl chloride in DMF and 1,2-dichloroethane to form the 4-chloro-dialkoxyquinazolines **8** and **9** in good yield.

A modified coupling procedure was employed for the production of the anilino- and benzylamino-quinazolines (Scheme 3). Anhydrous DMF was used as the reaction solvent instead of the previously reported isopropanol. The reaction was carried out at 80°C with nearly quantitative conversion to the substituted aminoquinazoline hydrochloride (HCl) salt within 30 min to 1 h depending on the aniline substituents. The precipitated HCl salt was filtered from the DMF solution and was converted to the free base for semi-preparative normal phase HPLC purification. The pure quinazolines were reconverted to the more stable HCl salt for the biological assays.

Chemical and physical data for all of the compounds is presented in Table 1. All of the anilino- and benzyl- quinazoline analogs were analyzed by analytical reversed-phase HPLC and found to be greater than 99% pure. Elemental analysis of all of the dialkoxyquinazoline analogs in Table 1 agree with the calculated values to within $\pm 0.4\%$

Lipophilicity measurement.

The lipophilicity of compounds can affect their tissue permeability properties that can impact their localization in target tissues. Lipophilicity may also affect binding to low affinity nonspecific sites that can compromise target tissue to background tissue ratios. The octanol/water partition coefficients of the quinazoline compounds were estimated by a reversed-phase HPLC method.⁴⁴ This method has been previously used by us to determine lipophilicities of steroid ligands.⁴⁵ The estimated Log $P_{o/w}$ values are reported in Table 1. The lipophilicities generally exhibited the expected trends with a couple of noted exceptions. The lipophilicity was greater for the diethoxy series relative to the corresponding dimethoxy analogs. Within the series **10a-d** and **11a-d** the lipophilicity increased with increasing size of the halogen from fluorine to iodine. Adding the trifluoromethyl moiety to **10a** and **11a** increased the lipophilicity by 1.7-1.8 log units. Interestingly, adding an extra methylene to produce the benzylamine did not significantly increase the compound lipophilicity (compare **14** and **16b**, **15** and **17b**). In contrast, the position of the fluorine on the aniline (C ring, Figure 1) ring did have a significant effect on the lipophilicity. The meta- and para- fluoroanilino analogs, **10a** and **16b**, had similar lipophilicities while

the ortho- substituted analog, **16a**, showed a 0.7 log unit decrease. This trend was similar for the dimethoxy analogs.

Biological Activity.

The sixteen quinazoline compounds were studied in a battery of *in vitro* assays to assess their biological properties and to develop a basis for screening these and future compounds for potential imaging agents. A radiometric binding assay was developed to determine the relative binding affinities of these compounds for the ATP binding site in the tyrosine kinase domain of the receptor. The ability of these molecules to inhibit EGFR tyrosine phosphorylation was probed. The specificity of a small subset of compounds was determined by assessing inhibition of ErbB2 and ErbB4 receptor phosphorylation. Finally, the ability of the ligand to inhibit cellular DNA synthesis, in cells dependent and not dependent on EGF for cell proliferation, was evaluated. This assay was performed in an effort to find a test that would be amenable to high throughput screening and whose results would potentially correlate with receptor binding and ultimately with the pharmacokinetic distribution of the tracer *in vivo*.

Receptor binding is a key characteristic that these molecules must possess to be suitable imaging agents. A receptor binding assay using EGF receptors extracted from the A431 human carcinoma cell membranes was developed and used to study the relative binding affinity of these compounds to the tyrosine kinase domain. Iodine-125 labeled **11d** (specific activity 583-596 Ci/mmol) was employed as the radioligand³⁶ and non-specific binding was determined by adding **11c**, the bromo- analog, to the assay. EGFR binding values, expressed as an IC₅₀, are shown in Table 2. All of the compounds demonstrated high affinity for the receptor with IC₅₀s ranging from 0.4 – 51 nM. In all cases the diethoxy analogs had relatively higher affinity for the receptor than the corresponding dimethoxy derivatives. Analogs **10b-10d** and **11b-11d**, the meta- chloro-, bromo- and iodo-anilino analogs, exhibited the highest relative affinities (nanomolar to subnanomolar) for the tyrosine kinase domain. Three fluoroanilino analogs, **10a**, **12**, and **16a** displayed relative affinities slightly less than 10 nM, generally considered the upper limit for imaging agents^{46,47}, while the remaining analogs had relative affinities greater than 16 nM.

While receptor binding is absolutely necessary for localization of a potential imaging agent, the ability to inhibit receptor function, in this case ligand-induced receptor tyrosine autophosphorylation, may be uncoupled from ligand binding. A series of assays were designed to examine the correlation between receptor binding and inhibition of receptor phosphorylation or inhibition of EGF-dependent DNA synthesis. The inhibition of ligand-induced EGFR tyrosine autophosphorylation is reported in Table 2. All of the compounds were potent inhibitors of EGFR tyrosine phosphorylation (kinase activity) with the exception of the 4-(3'-fluoro-5'-trifluoromethylanilino)-6,7-diethoxyquinazoline analog **12**. There was no correlation ($r^2 = 0.02$) between binding affinity and inhibition of ligand-induced EGFR tyrosine phosphorylation. Indeed, in contrast to the results of the receptor binding assay, in the EGFR tyrosine phosphorylation assays the diethoxy analogs were not consistently better inhibitors than the corresponding dimethoxy analogs.

Specificity for the EGF receptor versus other receptor tyrosine kinases, especially ErbB2 and ErbB4, is another desirable imaging characteristic. Thus, a small set of compounds was evaluated for inhibition of ligand-induced ErbB2 and ErbB4 tyrosine phosphorylation (kinase activity). The specificity of the compounds tested for EGFR appears to be high (Table 2). For the four compounds tested (**10c**, **10d**, **11c**, and **14**), the ErbB2 and ErbB4 tyrosine phosphorylation (kinase) IC_{50} values were at least one order of magnitude greater than the EGFR tyrosine phosphorylation (kinase) IC_{50} values. We do recognize that this is a comparison of phosphorylation inhibition rather than binding.

The specificity of the molecules for EGFR was also determined by examining their effect on DNA synthesis by the EGF-dependent MCF-10A human mammary epithelial cell line and the EGF-independent MCF-7 human mammary tumor cell line. These cell lines were treated with various concentrations of several of the compounds and DNA synthesis was measured by assaying 3H -thymidine incorporation. These data were used to calculate the DNA synthesis IC_{50} values for each compound in the two cell lines, shown in Table 3. The MCF7 DNA synthesis IC_{50} values for the compounds were at least one order of magnitude higher than the corresponding MCF10A DNA synthesis IC_{50} values. Because the DNA synthesis of MCF10A cells is EGF-dependent, these data suggest that the compounds inhibit MCF10A DNA synthesis by inhibiting the EGFR rather than some other target.

Discussion

There are four well-established criteria for the development of disease-specific radioprobes that would be sensitive to changes in binding site concentration.^{46,47} They are: i) identify a binding site whose concentration changes as a function of a specific disease; ii) design and produce a radioprobe that selectively targets the binding site; iii) evaluate sensitivity as a function of altered binding site concentration; and iv) evaluate sensitivity relative to the selected disease. The EGF receptor overexpression in various tumors satisfies the first criterion. Identifying lead molecules to test as imaging probes and developing an underlying selection process to identify future candidate molecules, the subject of the present effort, begins to address the second criterion.

Designing and producing an enzyme- or receptor-binding radioprobe involves several steps, often an iterative process, intended to obtain a thorough understanding of the biochemical and physiological behavior of the probe to match against a set of desirable imaging characteristics.^{46,47} A receptor-binding radiotracer should meet the following criteria: i) high affinity for the desired enzyme or receptor, typically <10 nM; ii) appropriate lipophilicity (coupled to cell membrane or blood-brain barrier penetration, typically 1.5 – 3.0); iii) high selectivity for the enzyme or receptor (e.g. low affinity for receptors within the same family or similar proteins, typically >10:1); iv) suitable metabolic properties (labeled metabolites can alter the distribution profile of the probe); and v) rapid clearance from non-target tissues and the body (necessary for good target-to-background ratio, typically >3:1 and lower radiation dose to the subject). *In vitro* data for a series of dialkoxyquinazoline EGFR-targeted compounds have been gathered and used to select probes for labeling and *in vivo* evaluation. These data were used to establish a ligand selection process. The process is detailed in the context of the following discussion.

The dialkoxyquinazolines (Figure 1) were chosen as the lead compounds in the present study based on the reported structure inhibition relationships.³³⁻³⁵ Fry and colleagues demonstrated that the quinazoline backbone and the 6,7-dimethoxy moieties were necessary for enhanced EGFR tyrosine kinase inhibition. The 6,7-diethoxy analog **10c** exhibited a four-fold lower inhibition IC₅₀ value (6 pM

vs 25 pM) and halogen substitution at the 2', 3', 4' and 5' positions, even 3', 4' dibromination, of the anilino ring ("C" ring Figure 1) was well tolerated. The fluorobenzylamino analog was not previously studied but based on the radiochemical availability of this analog it was included here.⁴⁸ The unsubstituted benzyl compound was evaluated as an inhibitor and found to have a 3 fold lower inhibition IC₅₀ value (10 nM) compared to the corresponding unsubstituted anilino compound (29 nM).^{33,35} The 3-fluoro-5-trifluoromethylaniline as well as 2-, 3- and 4- fluoroaniline can be synthesized with fluorine-18 so the corresponding non-radioactive analogs were added to the study.⁴⁹ Inhibition data from the 4-(3'-trifluoromethylanilino)-6,7-dimethoxyquinazoline (inhibition IC₅₀ = 0.24 nM) and the 3'-fluoroanilino analog (inhibition IC₅₀ = 3.8 nM) supported their inclusion.

The preparation of the analogs for this study was straightforward. The 4-chloro- dimethoxy- or diethoxy-quinazoline intermediates were synthesized and coupled with the appropriate aniline or benzylamine to yield the desired anilino- or benzylamino-quinazolines in good yield. The approach outlined herein improved upon the chemistry previously described by Bridges *et al.*³³ and provides a suitable starting point to generate libraries of anilino- or benzylamino- quinazolines with any dialkoxy or mixed alkoxy substituents in the 6 and 7 positions.

A receptor binding assay was developed to study the affinity of the compounds for the tyrosine kinase binding site and determine the correlation, if any, between binding and inhibition values. *In vitro* equilibrium binding assays provide a good means of segregating potential receptor-based imaging agents from those whose unfavorable kinetics (high binding potential, B_{max}/K_d) might lead to flow mediated distribution.⁴⁷ As all of the literature for the quinazolines and other classes of compounds targeting the EGFR tk reported inhibition constants, the following question was posed: Could these values be used as a primary determinant for potential imaging probes? All of the compounds possessed suitable affinity for the EGFR tk (IC₅₀ range = 0.4 - 51 nM). Likewise, all of the compounds were nM inhibitors of ligand-induced EGFR tyrosine phosphorylation (IC₅₀ range = 0.8 – 23.1 nM) in whole cells. Yet, there was a complete lack of correlation between the matched set of binding and phosphorylation data. Based on this small set of compounds the phosphorylation data may not be used to predict receptor affinity. This is likely due to the fact that inhibition of ligand-induced receptor phosphorylation is not

only a function of receptor binding affinity, but is also a function of the ability to penetrate a cell and gain access to the receptor. Thus, the receptor binding assay along with a measure of cell penetration (inhibition of EGFR dependent DNA synthesis, see below) will be integral as an initial screen for tracers. Compounds **10a-d**, **11b-d**, **12** and **16a** meet the generally accepted minimum affinity for receptor-based imaging agents, 10 nM.

A subsequent screen of selected lead compounds for the inhibition of ligand-induced tyrosine phosphorylation will identify those molecules that readily access the receptor. For example, compound **12** has a suitable affinity for EGFR *in vitro* but displays minimal inhibition of ligand-induced receptor tyrosine phosphorylation. Thus, compound **12** probably possesses limited penetration of cells and/or limited EGFR access. Therefore, compound **12** is likely to be of limited value as a potential EGFR-specific tumor imaging agent. Compounds **10a-d**, **11b-d**, and **16a** are potent inhibitors of EGFR phosphorylation.

In cases where facilitated transport is nonexistent cell membrane permeability is a direct function of the diffusion coefficient and compound lipophilicity. If the partition coefficient value is too low, the compound will not cross a cell membrane; if the value is too high, hydrophobic interactions with lipids and proteins will dominate, leading to high non-specific binding, compromising image contrast. It has been demonstrated for radiotracers crossing the blood-brain barrier that a Log $P_{o/w}$ range of 1.5 – 3 is optimal.⁵⁶ While this range works equally well for non-brain receptor-targeted tracers, estrogen radioprobes with higher lipophilicity (up to Log P = 4.5) have been successful tumor imaging agents.⁵⁷ Therefore, the Log $P_{o/w}$ range for the selection of the EGFR probes in the current study has been set from 1.5 to 4. The HPLC derived lipophilicities (Log $P_{o/w}$) ranged from 2.2 to 5.5. Of those compounds previously chosen, **10a** and **11b-d** and **16a** fall within this desired range.

Selectivity for the chosen receptor is the final *in vitro* test. One preliminary measure of receptor selectivity that was employed in this study was to evaluate ErbB2 and ErbB4 inhibition. All of the compounds were much less potent inhibitors of ligand-induced ErbB2 and ErbB4 phosphorylation than of ligand-induced EGFR phosphorylation. Indeed the compounds tested here exhibit between one and two orders of magnitude of selectivity for the EGFR over ErbB2 or ErbB4. All of the compounds tested

may be reasonable EGFR-selective tumor imaging agents. The optimal agent would exhibit the least amount of avidity for other RTKs. In many types of tumor cells ErbB2 is frequently overexpressed at levels comparable to the levels of EGFR overexpression.⁷ Similarly, ErbB4 is expressed in the normal mammary epithelium⁵⁹ and infrequently overexpressed in tumor tissue.^{58, 59} These observations highlight the need for EGFR-selective imaging agents that exhibit minimal binding to ErbB2 and ErbB4, among other RTKs, in order to determine and understand EGFR expression using molecular imaging techniques.

The quinazoline compounds were also assayed for inhibition of cellular DNA synthesis in EGF-dependent (MCF10A) and EGF-independent (MCF7) cell lines. This assay, like the inhibition of ligand-induced receptor tyrosine phosphorylation assays, not only assesses the specificity of a compound for EGFR, but also provides a measure of a compounds ability to penetrate cells and specifically target the EGFR. Thus, it is not surprising that compound **12**, which we hypothesized failed to inhibit ligand-induced EGFR tyrosine phosphorylation because it exhibits limited cell penetration, also failed to inhibit EGF-dependent and –independent DNA synthesis.

In general, the MCF10A DNA synthesis IC₅₀ values are much lower than the MCF7 DNA synthesis IC₅₀ values. This suggests that the compounds inhibit DNA synthesis in the MCF10A cells by primarily targeting EGFR. Indeed, this assay has been used to connote that Lavendustin A analogs, which inhibit EGFR kinase activity, inhibit cell proliferation by inhibiting tubulin polymerization.⁵⁰ This indicates that at least some of the compounds inhibit DNA synthesis in the MCF7 cells by targeting a protein other than the EGFR. Compounds that may target ATPases other than the EGFR would be expected to exhibit reduced MCF7/MCF10A DNA synthesis IC₅₀ ratios. Compounds with reduced ratios include **11d**, **13**, and **17b**. Such molecules may not be specific for the EGFR and may not be appropriate for further investigation as potential EGFR-specific tumor imaging agents. Compounds **10a-d**, **11b,c**, **14**, **16a,b** and **17a** exhibit elevated MCF7/MCF10A DNA synthesis IC₅₀ ratios and by this criterion may be suitable for further investigation as a potential EGFR-specific tumor imaging agents.

These criteria taken together support the further investigation of compounds **10a**, **11b**, **11c** and **16a**. Compounds **10a**, 4-(3'-fluoroanilino)- and **16a**, 4-(2'-fluoroanilino)-6,7-diethoxyquinazoline, may

both be labeled with the 110 min half-life fluorine-18. Compound **11b**, 4-(3'-chloroanilino)-6,7-dimethoxyquinazoline may be labeled with the 20 min half-life carbon-11; however, as pointed out earlier, the short half-life may not afford the time necessary to achieve the desired imaging pharmacokinetics. Compound **11c** 4-(3'-bromoaniline)-6,7-dimethoxyquinaxoline may be a candidate for bromine-76 (16.2h positron emitter) labeling.

Interestingly, Bonasera et al.³⁸, have recently labeled three of the analogs studied in this paper, **11a**, **13** and **17b**, and injected one of them, **17b**, into A431 tumor-bearing mice. Compound **13** was not studied *in vivo* due to low measured EGFR inhibition values and compound **11a** was not readily labeled with fluorine-18. Tumor uptake of [¹⁸F]**17b** at 30 minutes was greater than 1% of the injected dose per gram (%ID/g) of tissue but the tumor to blood ratio was only 0.6. At 60 minutes the tumor uptake rose slightly to 1.34 %ID/g with a tumor to blood ratio of 1.62. This uptake may be associated with EGFR targeting but receptor blocking studies were not performed to demonstrate receptor mediated uptake. Bone uptake, an indicator of metabolic defluorination, was also not assessed. A second fluorine-labeled analog, 4-(3', 4'- dichloro-6'-fluoroanilino)-6,7-dimethoxyquinazoline, was tested in tumor-bearing mice. Tumor accumulation of the probe never exceeded blood levels and the uptake was not receptor-mediated. Several factors may have contributed to the limited tumor accumulation *in vivo* including high non-specific binding or diminished availability due to untoward metabolism.

It is clear from the preliminary studies that development of an effective EGFR imaging probe may present some challenges. Thus, effective screening of candidate probes and establishment of baseline data is essential for a radiopharmaceutical development program targeting EGFR.

Conclusion

Anilino-dialkoxyquinazolines suitable for labeling with radioisotopes were readily prepared using an approach amenable to a synthetic library of amino-quinazoline analogs. All of the dialkoxy analogs possessed suitable affinity for the EGF receptor and all analogs were potent inhibitors of ligand-induced EGFR phosphorylation. They exhibited a range of lipophilicities based on the A ring and C ring substituents. Selectivity, as determined by comparison of ErbB2 and ErbB4 receptor inhibition to EGFR inhibition, favored the EGFR by 1-2 orders of magnitude. Based on measures of affinity, lipophilicity

and selectivity, analogs **10a**, **11b**, **11c** and **16a**, were selected for further evaluation as tumor imaging probes.

Experimental Section

Chemistry. Unless otherwise noted, all solvents and reagents were obtained from commercial suppliers (Aldrich Chemical, Co., Lancaster Synthesis, Inc., VWR, *etc.*) and were used without further purification. Melting points were determined using a Mel-Temp melting point apparatus and are reported uncorrected. NMR spectra were recorded on either a Bruker VBAMX 300 300 MHz or AMX 400 400 MHz. Chemical shifts are reported in ppm (δ) relative to an internal standard. Elemental analyses were performed by the Microanalytical Laboratory in the College of Chemistry, University of California, Berkeley. Mass spectral data was obtained on a Perkin Elmer SCIEX mass spectrometer at the SynPep Corporation facility (Dublin, CA) or on a VG ProSpec mass spectrometer at the Mass Spectrometry Facility in the College of Chemistry, University of California, Berkeley.

2-nitro-4,5-diethoxybenzoic acid (2). A flask immersed in a room-temperature water bath was charged with 3,4-diethoxybenzoic acid **1** (12.9 g, 61.4 mmol) and acetic acid (glacial, 52 mL). Over a 15 min. period HNO₃ (70%, 54 mL) was added dropwise with stirring. The deep orange solution was stirred for an additional 125 min. at room temperature. The reaction was quenched upon addition of 110 g of ice. A yellow precipitate formed, which was filtered and washed with H₂O (3 x 50 mL). The resulting yellow-white solid was dissolved in ether (150 mL). The ether was washed with 1N NaOH (3 x 60 mL). The aqueous washings were combined, and acidified with concentrated HCl resulting in the production of a pale yellow precipitate. The precipitate was filtered, washed with H₂O (3 x 100 mL) and dissolved in ether. The ether was dried over MgSO₄, and concentrated in vacuo to yield 10.55g (67%) of **2**. mp 142-145 °C; ¹H-NMR (CDCl₃): δ 7.36 (s, 1H, *H*-6), 7.21 (s, 1H, *H*-3), 4.20 (q, 2H, CH₂CH₃, J = 6.9 Hz), 4.17 (q, 2H, CH₂CH₃, J = 6.9 Hz), 1.50 (t, 6H, CH₂CH₃, J = 7.1 Hz). EI MS [M⁺] 255 (100).

2-amino-4,5-diethoxybenzoic acid (4). **a)** A round-bottom flask containing 2-amino-4,5-diethoxymethyl benzoate **3** (1.00 g, 4.19 mmol, Sigma-Aldrich Rare Chemicals) was mixed with 6.25N NaOH (2.67 mL, 16.7 mmol) and water (5.0 mL). The solution was refluxed for one hour to give a clear brown

solution. After cooling at ambient temperature for 10 minutes, water (15 mL) was added to the flask and the solution was titrated to pH 6 with 1N HCl. The solution was further cooled in an ice bath for 30 minutes. The precipitate was filtered, washed with water (100 mL) and pentanes (50 mL) and dried in vacuo over P₂O₅ overnight to give 0.83 g (76%) of 2-amino-4,5-diethoxybenzoic acid as a pale yellow solid.

b) An oven-dried round-bottomed flask (250 mL) equipped with a stirring bar was immersed in a room-temperature water bath and charged with SnCl₂•2H₂O (24.9 g, 110 mmol) and HCl (conc., 100 mL). 2-Nitro-4,5-diethoxybenzoic acid **2** (1.64 g, 6.43 mmol) was added and the mixture was stirred for 120 min. at room temperature. The mixture was diluted with HCl (conc., 40 mL), filtered, and washed with conc. HCl. The resulting white solid was taken up in H₂O (500 mL) and filtered to remove the remaining undissolved material. The pH of the filtrate was adjusted to 4.5 using NH₄OH. The deep purple solution was extracted with CH₂Cl₂ (3 x 300 mL). The organic washings were combined, dried over MgSO₄, and concentrated in vacuo, to yield 0.64 g (44%) of a purple-white powder.

mp 120-126 °C; ¹H NMR (CDCl₃): δ 7.37 (s, 1H, *H*-6), 6.11 (s, 1H, *H*-3), 4.06 (q, 2H, CH₂CH₃, J = 6.8 Hz), 4.01 (q, 2H, CH₂CH₃, J = 6.8 Hz), 1.46 (t, 3H, CH₂CH₃, J = 6.8 Hz), 1.41 (t, 3H, CH₂CH₃, J = 6.8 Hz). EI MS [M⁺] 225 (100).

6,7-diethoxyquinazolin-4-one (6). A modified literature procedure³³ was developed to produce **6**. A 500 mL round bottom flask equipped with an air condenser was charged with 2-amino-4,5-diethoxybenzoic acid **4** (1.36 g, 6.04 mmol) and formamidine hydrochloride (0.70 g, 8.76 mmol). The solids were thoroughly mixed then heated to 200 °C under an argon atmosphere for 15 minutes. The heating block temperature was adjusted to 80 °C and the solution cooled to 80 °C over 40 minutes. Dilute NaOH (0.33N, 20 mL) was added to the flask. The mixture was sonicated at room temperature for 1 hour producing in a dark gray-purple suspension. The solid was filtered, washed with water (200

mL), pentanes (200 mL), and ethyl acetate (200 mL) to give 6,7-diethoxyquinazolin-4-one as an off-white solid. Drying *in vacuo* overnight over P₂O₅ gave 0.80 g (57%) of **6**. mp 248-251.5 °C; ¹H-NMR (CD₃OD): δ 7.98 (s, 1H, ArH), 7.55 (s, 1H, ArH), 7.11 (s, 1H, ArH), 4.20 (q, 2H, CH₂CH₃, J = 6.8 Hz), 4.16 (q, 2H, CH₂CH₃, J = 6.8 Hz), 1.48 (t, 3H, CH₂CH₃, J = 6.8 Hz), 1.46 (t, 3H, CH₂CH₃, J = 6.8 Hz). EI MS [M⁺] 234 (100).

6,7-dimethoxyquinazolin-4-one (7). 2-amino-4,5-dimethoxybenzoic acid **5** (5.0 g, 25.3 mmol) was converted to **7** in 65% yield (3.64 g) following the procedure for compound **6**. mp 278-278.5 °C; (lit.³³ mp 295-298 °C) ¹H-NMR [(CD₃)₂SO]: δ 12.07 (br s, 1H, NH), 7.98 (s, 1H, ArH), 7.43 (s, 1H, ArH), 7.11 (s, 1H, ArH), 3.90 (s, 3H, OCH₃), 3.87 (s, 3H, OCH₃).

4-chloro-6,7-diethoxyquinazoline (8). Following a modified literature procedure³³, DMF (0.94 mL, 12.1 mmol) was added dropwise to a solution of 1,2-dichloroethane (8.1 mL) and oxalyl chloride (1.1 mL, 12.6 mmol) stirring under argon, vigorously releasing gas. Following cessation of the gas production, 6,7-diethoxyquinazolin-4-one **6** (1.89 g, 8.1 mmol) was added to the thick white slurry then refluxed for 2.5 hours, resulting in a yellow-brown suspension. The reaction was quenched by addition of Na₂HPO₄ (0.5M, 16.8 mL) followed by stirring in an ice bath for 1 hour. The suspension was filtered and washed with water (200 mL) to isolate 4-chloro-6,7-diethoxyquinazoline **8** as a pale gray solid, 1.48 g (73%). mp 139-140 °C; ¹H-NMR (CDCl₃): δ 8.82 (s, 1H, ArH), 7.35 (s, 1H, ArH), 7.28 (s, 1H, ArH), 4.26 (m, 4H, OCH₂CH₃), 1.55 (m, 6H, OCH₂CH₃). APCI MS [M+1] 253.1 (100), 255.1 (33). Anal. (C₁₂H₁₃ClN₂O₂) C, H, N.

4-chloro-6,7-dimethoxyquinazoline (9). 6,7-dimethoxyquinazolin-4-one **7** (3.40 g, 16.5 mmol) was converted to **9** in 52% yield (1.91 g) following the procedure for compound **8**. mp 184-186 °C; ¹H-NMR (CDCl₃): δ 8.86 (s, 1H, ArH), 7.38 (s, 1H, ArH), 7.32 (s, 1H, ArH), 4.05 (s, 6H, OCH₃). APCI MS [M+1] 225.1 (100), 227.1 (30). Anal. (C₁₀H₉ClN₂O₂) C, H, N.

4-(3'-chloroanilino)-6,7-diethoxyquinazoline hydrochloride (10b): General coupling procedure. A solution of 4-chloro-6,7-diethoxyquinazoline **8** (71 mg, 0.32 mmol) and 3-chloroaniline (40 μ L, 0.38 mmol) in 3 mL of DMF was heated at 80 °C under argon for 40 min. The reaction was cooled at room temperature for 1 hour. Ethyl acetate (2 mL) was added. The resulting precipitate was filtered and further washed with 20 mL of ethyl acetate to give the HCl salt 10a, 100 mg (90%). The salt was converted to the free base by dissolving **10b** in a mixture of 3 mL of ethyl acetate and 3 mL of 1N NaOH. The biphasic mixture was stirred vigorously for several minutes. The ethyl acetate layer was filtered, washed with water (3 x 1mL) and dried over MgSO₄. The ethyl acetate was filtered and the volume was reduced to less than 1 mL. The solution was applied to a normal phase semi-preparative HPLC (Whatman M9/50 partisil 10 column, 70:30 EtOAc: hexane, 6 mL/min., UV 254 nm) for purification. The fraction containing the free base was concentrated to dryness and the residue was dissolved in MeOH (8 mL) with gentle heating. HCl (1N, 3 mL) was added and the solution was placed in an ice bath. The precipitate was filtered and washed with ethyl acetate to give 72 mg (65%) of the 4-(3-chloroanilino)-6,7-diethoxyquinazoline hydrochloride salt **10b**. mp 260-261 °C; ¹H NMR (CD₃OD) δ 8.72 (s, 1H, *H*-2), 7.97 (s, 1H, *Ar-H*), 7.87 (s, 1H, *H*-2'), 7.65 (d, 1H, *H*-4', *J* = 8.0 Hz), 7.47 (t, 1H, *H*-5' *J* = 8.1 Hz), 7.35 (d, 1H, *H*-6', *J* = 8.0 Hz), 7.20 (s, 1H, *Ar-H*), 4.31 (q, 4H, OCH₂CH₃, *J* = 6.9 Hz), 1.55 (t, 6H, OCH₂CH₃, *J* = 7.0 Hz). EI MS [*M*+][•] 343 (100), 345 (34). Anal. (C₁₈H₁₈ClN₃O₂) C, H, N.

4-(3'-fluoroanilino)-6,7-diethoxyquinazoline hydrochloride (10a). Similar treatment of **8** (0.021g, 0.083 mmol) with 3-fluoroaniline yielded **10a** (77%). mp 247.0-248.0 °C; ¹H-NMR (CD₃OD): δ 8.73 (s, 1H, *H*-2), 7.99 (s, 1H, *H*-5), 7.66 (d, *J*=10.6 Hz, 1H, *H*-2'), 7.53 (m, 1H, *H*-5'), 7.53 (m, 1H, *H*-6'), 7.21 (s, 1H, *H*-8), 7.08 (dd, *J*=9.1, 7.1 Hz, 1H, *H*-4'), 4.33 (q, *J*=6.9 Hz, 4H, CH₃CH₂O), 1.55 (t, *J*=6.9 Hz, 3H, CH₃CH₂O), 1.54 (t, *J*=6.9 Hz, 3H, CH₃CH₂O). EI MS [*M*] 327. Anal. (C₁₈H₁₈FN₃O₂•HCl) C, H, N.

4-(3'-bromoanilino)-6,7-diethoxyquinazoline hydrochloride (10c). Similar treatment of **8** (59.5 mg, 0.24 mmol) with 3-bromoaniline yielded **10c** (50%) mp 250-252 °C (Lit.³³ mp 155-167 °C— free base). ¹H NMR [(CD₃)₂SO] δ 11.17 (br s, 1H, *NH*), 8.86 (s, 1H, *H*-2), 8.19 (s, 1H, *Ar-H*), 7.99 (s, 1H, *H*-2'),

7.73 (d, 1H, *H*-4', *J* = 7.6 Hz), 7.51 (d, 1H, *H*-6', *J* = 7.5 Hz), 7.45 (t, 1H, *H*-5' *J* = 8.0 Hz), 7.23 (s, 1H, *Ar*-*H*), 4.27 (m, 4H, OCH₂CH₃, *J* = 7.2 Hz), 1.45 (t, 6H, OCH₂CH₃, *J* = 6.8 Hz). HREIMS Calc for C₁₈H₁₈BrN₃O₂ *m/z* (M⁺) 387.05824, 389.05619 found 387.05776 , 389.05532 Anal. (C₁₈H₁₈BrN₃O₂) C,H,N.

4-(3'-iodoanilino)-6,7-diethoxyquinazoline hydrochloride (10d). Similar treatment of **8** (116.1 mg, 0.46 mmol) with 3-iodoaniline yielded **10d** (95%). mp 258.5-261 °C; ¹H NMR [(CD₃)₂SO] δ 11.19 (br s, 1H, *NH*), 8.86 (s, 1H, *H*-2), 8.19 (s, 1H, *Ar*-*H*), 8.10 (s, 1H, *H*-2'), 7.75 (d, 1H, *H*-4', *J* = 8.0 Hz), 7.67 (d, 1H, *H*-6', *J* = 8.0 Hz), 7.30 (s, 1H, *Ar*-*H*), 7.29 (t, 1H, *H*-5' *J* = 8.0 Hz), 4.27 (m, 4H, OCH₂CH₃), 1.44 (t, 6H, OCH₂CH₃, *J* = 6.8 Hz). APCI MS [M+1] 436.0 (100). Anal. (C₁₈H₁₈IN₃O₂•HCl) C,H,N.

4-(3'-fluoroanilino)-6,7-dimethoxyquinazoline hydrochloride (11a). Similar treatment of **9** (0.032g, 0.14 mmol) with 3-fluoroaniline yielded **11a** (27%). mp 244.5-246.0 °C (Lit.³³ mp 253-254 °C); ¹H-NMR (CD₃OD): δ 8.72 (s, 1H, *H*-2), 7.82 (s, 1H, *H*-5), 7.47 (d, *J*=10.6 Hz, 1H, *H*-2'), 7.33 (m, 1H, *H*-5'), 7.33 (m, 1H, *H*-6'), 7.03 (s, 1H, *H*-8), 6.89 (dd, *J*=8.6, 7.3 Hz, 1H, *H*-4'), 3.88 (s, 6H, CH₃O). EI MS [M] 299. Anal. (C₁₆H₁₄FN₃O₂•1.1HCl) C,H,N.

4-(3'-chloroanilino)-6,7-dimethoxyquinazoline hydrochloride (11b). Similar treatment of **9** (71.1 mg, 0.32 mmol) with 3-chloroaniline yielded **11b** (90%), mp 230-235 °C, (Lit.³³ mp 261-262 °C); ¹H NMR (CD₃OD) δ 8.66 (s, 1H, *H*-2), 7.93 (s, 1H, *Ar*-*H*), 7.90 (s, 1H, *H*-2'), 7.66 (d, 1H, *H*-4', *J* = 8.0 Hz), 7.44 (t, 1H, *H*-5' *J* = 8.1 Hz), 7.29 (d, 1H, *H*-6', *J* = 8.0 Hz), 7.21 (s, 1H, *Ar*-*H*), 4.02 (s, 6H, OCH₃). HREIMS Calc for C₁₆H₁₄ClN₃O₂ *m/z* (M⁺) 315.07745, 317.07450 found 315.07682 , 317.07303. Anal. (C₁₆H₁₄ClN₃O₂•HCl) C,H,N.

4-(3'-bromoanilino)-6,7-dimethoxyquinazoline hydrochloride (11c). Similar treatment of **9** (312 mg, 1.39 mmol) with 3-bromoaniline yielded **11c** (87%). mp 256-257.5 °C; ¹H NMR [(CD₃)₂SO] δ 11.35 (br s, 1H, *NH*), 8.88 (s, 1H, *H*-2), 8.29 (s, 1H, *Ar*-*H*), 8.01 (s, 1H, *H*-2'), 7.77 (d, 1H, *H*-4', *J* = 8.0 Hz), 7.50

(d, 1H, *H*-6', *J* = 8.0 Hz), 7.45 (t, 1H, *H*-5' *J* = 8.0 Hz), 7.32 (s, 1H, Ar-*H*), 4.00 (s, 3H, OCH₃), 3.99 (s, 3H, OCH₃). EI MS [*M*+] 359 (100), 361 (97). Anal. (C₁₆H₁₄BrN₃O₂•HCl) C, H, N.

4-(3'-iodoanilino)-6,7-dimethoxyquinazoline hydrochloride (11d). Similar treatment of **9** (276 mg, 1.23 mmol) with 3-iodoaniline yielded **11d** (92%). mp 251-251.5 °C (Lit.³³ mp 273 °C). ¹H NMR [(CD₃)₂SO] δ 11.33 (br s, 1H, NH), 8.90 (s, 1H, *H*-2), 8.30 (s, 1H, Ar-*H*), 8.28 (s, 1H, *H*-2'), 7.79 (d, 1H, *H*-4', *J* = 8.0 Hz), 7.69 (d, 1H, *H*-6', *J* = 8.0 Hz), 7.35 (s, 1H, Ar-*H*), 7.31 (t, 1H, *H*-5' *J* = 8.0 Hz), 4.04 (s, 3H, OCH₃), 4.02 (s, 3H, OCH₃). APCI MS [*M*+1] 408.0 (100). Anal. (C₁₆H₁₄IN₃O₂•HCl) C, H, N.

4-(3'-fluoro-5'-trifluoromethylanilino)-6,7-diethoxyquinazoline hydrochloride (12). Similar treatment of **8** (58.5 mg, 0.23 mmol) with 3-fluoro-5-trifluoromethylaniline yielded **12** (92%). mp 278-280 °C; ¹H NMR (CDCl₃) δ 8.70 (s, 1H, *H*-2), 8.09 (d, 1H, *H*-4', *J*_{H,F} = 10.9), 7.62 (s, 1H, Ar-*H*), 7.26 (s, 1H, *H*-6'), 7.22 (br s, 1H, NH), 7.06 (d, 1H, *H*-2', *J*_{H,F} = 8.0 Hz), 7.00 (s, 1H, Ar-*H*), 4.24 (m, 4H, OCH₂CH₃), 1.55 (m, 6H, OCH₂CH₃). HREIMS Calc for C₁₉H₁₇F₄N₃O₂ *m/z* (*M*+) 395.12569 found 395.12596. Anal. (C₁₉H₁₇F₄N₃O₂•HCl) C, H, N.

4-(3'-fluoro-5'-trifluoromethylanilino)-6,7-dimethoxyquinazoline hydrochloride (13). Similar treatment of **9** (150 mg, 0.67 mmol) with 3-fluoro-5-trifluoromethylaniline yielded **13** (19%). mp 269-270.5 °C; ¹H NMR (CDCl₃) δ 8.72 (s, 1H, *H*-2), 8.08 (d, 1H, *H*-4', *J*_{H,F} = 10.8), 7.63 (s, 1H, Ar-*H*), 7.38 (br s, 1H, NH), 7.27 (s, 1H, *H*-6'), 7.06 (d, 1H, *H*-2', *J*_{H,F} = 8.4 Hz), 7.02 (s, 1H, Ar-*H*), 4.03 (s, 3H, OCH₃), 4.01 (s, 3H, OCH₃). APCI MS [*M*+1] 368.1 (100). Anal. (C₁₇H₁₃F₄N₃O₂•HCl) C, H, N.

4-[(4'-fluorobenzyl)amino]-6,7-diethoxyquinazoline hydrochloride (14). Similar treatment of **8** (66.9 mg, 0.26 mmol) with 4-fluorobenzylamine yielded **14** (84%). mp 238.5-240 °C; ¹H NMR (CDCl₃) δ 8.56 (s, 1H, *H*-2), 7.37 (dd, 2H, *H*-2',*H*-6', *J*_{H,H} = 8.2, *J*_{H,F} = 5.5), 7.18 (s, 1H, Ar-*H*), 7.03 (t, 2H, *H*-3', *H*-5', *J*_{H,F} = *J*_{H,H} = 8.6 Hz), 6.84 (s, 1H, Ar-*H*), 5.53 (br s, 1H, NH), 4.81 (d, 2H, -CH₂-, *J* = 5.4), 4.20 (q,

2H, OCH₂CH₃, J = 7.0 Hz), 4.12 (q, 2H, OCH₂CH₃, J = 7.0 Hz), 1.51 (t, 3H, OCH₂CH₃, J = 7.0 Hz), 1.49 (t, 3H, OCH₂CH₃, J = 7.0 Hz). EI MS [M+1] 341 (100). Anal. (C₁₉H₂₀FN₃O₂) C,H,N.

4-[(4'-fluorobenzyl)amino]-6,7-dimethoxyquinazoline hydrochloride (15). Similar treatment of **9** (320 mg, 0.143 mmol) with 4-fluorobenzylamine yielded **15** (22%). mp 250-251 °C; ¹H NMR [(CD₃)₂SO] δ 10.37 (br s, 1H, NH), 8.82 (s, 1H, H-2), 8.00 (s, 1H, Ar-H), 7.45 (dd, 2H, H-2',H-6', J_{H,H} = 8.4, J_{H,F} = 5.6), 7.22 (s, 1H, Ar-H), 7.19 (t, 2H, H-3', H-5', J_{H,F} = J_{H,F} = 8.8 Hz), 4.91 (d, 2H, -CH₂-, J = 5.2), 3.95 (s, 3H, OCH₃), 3.94 (s, 3H, OCH₃). APCI MS [M+1] 314.2 (100). Anal. (C₁₇H₁₆FN₃O₂•HCl) C,H,N.

4-(2'-fluoroanilino)-6,7-diethoxyquinazoline hydrochloride (16a). Similar treatment of **8** (0.024g, 0.095 mmol) 2-fluoroaniline yielded **16a** (61%). mp 220.5-222.0 °C; ¹H-NMR (CD₃OD): δ 8.62 (s, 1H, H-2), 7.91 (s, 1H, H-5), 7.57 (dd, J=7.7, 7.5 Hz, 1H, H-5'), 7.44 (m, 1H, H-4'), 7.32 (d, J=7.7 Hz, 1H, H-6'), 7.28 (m, 1H, H-3'), 7.20 (s, 1H, H-8), 4.32 (q, J=6.6 Hz, 2H, CH₃CH₂O), 4.29 (q, J=6.6 Hz, 2H, CH₃CH₂O), 1.55 (t, J=6.6 Hz, 3H, CH₃CH₂O), 1.54 (t, J=6.6 Hz, 3H, CH₃CH₂O). HREIMS Calc for C₁₈H₁₈FN₃O₂ m/z (M+) 327.13831 found 327.13779. Anal. (C₁₈H₁₈FN₃O₂•1.4HCl) C,H,N.

4-(4'-fluoroanilino)-6,7-diethoxyquinazoline hydrochloride (16b). Similar treatment of **8** (0.10 g, 0.40 mmol) with 4-fluoroaniline yielded **16b** (97%). mp 252.0-255.0 °C; ¹H-NMR ((CD₃)₂SO): δ 10.06 (s, 1H, NH), 8.77 (d, J=1.8 Hz, 1H, H-2), 8.27 (s, 1H, H-5), 7.68 (m, 2H, H-2', H-6'), 7.32 (s, 1H, H-8), 7.29 (dd, J=6.7, 6.6 Hz, 2H, H-3', H-5'), 4.25 (q, J=5.1 Hz, 2H, CH₃CH₂O), 4.20 (q, J=5.1 Hz, 2H, CH₃CH₂O), 1.41 (t, J=5.1 Hz, 3H, CH₃CH₂O), 1.40 (t, J=5.1 Hz, 3H, CH₃CH₂O). APCI MS [M+1] 328.3. Anal. (C₁₈H₁₈FN₃O₂•HCl) C,H,N.

4-(2'-fluoroanilino)-6,7-dimethoxyquinazoline hydrochloride (17a). Similar treatment of **9** (0.033g, 0.15 mmol) with 2-fluoroaniline yielded **17a** (50%). mp 231.0-232.0 °C; ¹H-NMR (CD₃OD): δ 8.65 (s,

1H, *H*-2), 7.97 (s, 1H, *H*-5), 7.58 (ddd, *J*=7.7, 7.5 Hz, 1.10 Hz, 1H, *H*-5'), 7.44 (m, 1H, *H*-4'), 7.33 (d, *J*=7.7 Hz, 1H, *H*-6'), 7.29 (m, 1H, *H*-3'), 7.25 (s, 1H, *H*-8), 4.09 (s, 3H, CH₃O), 4.07 (s, 3H, CH₃O). HREIMS Calc for C₁₆H₁₄FN₃O₂ *m/z* (M⁺) 299.10701 found 299.10648. Anal. (C₁₆H₁₄FN₃O₂•HCl) C, H, N.

4-(4'-fluoroanilino)-6,7-dimethoxyquinazoline hydrochloride (17b). Similar treatment of **9** (0.10 g, 0.45 mmol) with 4-fluoroaniline yielded **17b** (94%). mp 247.0-248.0 °C; ¹H-NMR ((CD₃)₂SO): δ 10.12 (br. s, 1H, NH), 8.79 (s, 1H, *H*-2), 8.25 (s, 1H, *H*-5), 7.68 (m, 2H, *H*-2', *H*-6'), 7.30 (dd, *J*=7.0, 6.2 Hz, 2H, *H*-3', *H*-5'), 7.30 (s, 1H, *H*-8), 3.98 (s, 3H, CH₃O), 3.96 (s, 3H, CH₃O). APCI MS [M+1] 300.1. Anal. (C₁₆H₁₄FN₃O₂•HCl) C, H, N.

Log P Determinations. Log P values were estimated from the log *k'*_w values determined by HPLC chromatography following the procedure of Minick.⁴⁴ The solvents were HPLC grade methanol, 1-octanol, *n*-decylamine and distilled deionized water. The standards (p-anisidine [0.95]; acetophenone [1.58]; p-bromoaniline [2.26]; naphthalene [3.30]; pyrene [4.88]) were obtained from Aldrich and used without further purification. A ThermoQuest HPLC system equipped with an autoinjector, pump, diode-array UV/Vis detector and an Es Industries MC8 column (4.6 x 150 mm, 5μ, 60Å) was used for these measurements. The organic mobile phase was methanol containing 0.25% v/v 1-octanol. The aqueous mobile phase was octanol saturated water containing 0.02 M 3-morpholinopropanesulfonic acid (MOPS) buffer, 0.15% v/v *n*-decylamine, adjusted to pH 7.4. The flow rate was set at 1 mL/min. The quinazolines and standards were dissolved in methanol to a final concentration of approximately 0.1 mg/mL and 10 μL was injected onto the column. The column void volume was estimated from the retention time of uracil, which was included as a non-retained internal reference standard with each injection.

The log k'_w was determined by linear extrapolation of the compound residence time (retention volume less void volume) versus the methanol concentration over a range of 60 to 85% methanol mobile phase.

Biological Methods.

Cell Lines and Cell Culture. The CEM human T lymphocyte cell line engineered to express ErbB4 (CEM/4) and its culture conditions have been described previously.^{51,52} Briefly, these cells were propagated in RPMI supplemented with 10% heat-inactivated fetal bovine serum and 300 $\mu\text{g/ml}$ G418. The BaF3 mouse lymphoid cell lines engineered to express either EGFR (BaF3/EGFR) or ErbB2 and ErbB3 together (BaF3/2+3) and the culture conditions for these cell lines have been described earlier.⁵³ Briefly, these cells were propagated in RPMI supplemented with 10% fetal bovine serum, 300 $\mu\text{g/ml}$ G418, and 10% medium conditioned by WeHI cells. This conditioned medium serves as a source for Interleukin 3.

MCF-10A human mammary epithelial cells and MCF-7, MDA-MB-231, and MDA-MB-453 human mammary tumor cell lines were obtained from the American Type Culture Collection (ATCC). These lines were propagated according to ATCC recommendations.

Inhibition of Receptor Tyrosine Phosphorylation. The assay for inhibition of ErbB family receptor tyrosine phosphorylation was adapted from a previously-described protocol.^{52,53} Briefly, 200 mL cultures of CEM/4, BaF3/EGFR, or BaF3/2+3 cells were grown to saturation density ($\sim 10^6$ cells/mL) and were incubated for 24 hours at 37°C in serum-free medium to reduce basal levels of receptor tyrosine phosphorylation. The cells were collected by centrifugation and resuspended in serum-free medium at a final concentration of $\sim 10^7$ cells/mL (~ 20 mL of cells). Cells were transferred to microcentrifuge tubes in 1 mL aliquots and putative kinase inhibitors were added to the cells. Each tyrosine kinase inhibitor was tested at 3-5 different concentrations. The inhibitors were dissolved in 5 μL DMSO; hence, cells treated with 5 μL DMSO were used as a solvent control. Cells were incubated

in the presence of inhibitor for 2 hours at 37°C, then were incubated on ice for 20 minutes. Chilling the cells reduces the amount of ligand-induced receptor downregulation.⁵³

Ligand was then added to the appropriate samples at a final concentration of 100 ng/mL and the samples were mixed and incubated on ice for 7 minutes. Recombinant human Epidermal growth factor (EGF - Sigma) was used as the ligand for EGFR, whereas Neuregulin1 β (NRG1 β – R&D Systems) was used as the ligand for ErbB3 and ErbB4. Note that because ErbB3 lacks kinase activity, ligand-induced ErbB2 and ErbB3 phosphorylation in the BaF3/2+3 cells is the result of ligand-induced ErbB2-ErbB3 heterodimerization and ErbB2 kinase activity.⁵³ Following incubation with ligand, the cells were collected by centrifugation, the supernatant was removed by aspiration, and the cells were resuspended in an isotonic lysis buffer containing 0.5% NP40/Igepal CA-630 (non-ionic detergent - Sigma).

The cells were incubated for 20 minutes on ice to permit lysis. The samples were centrifuged for 10 minutes at 4°C to collect the nuclei and cellular debris. The supernatants (cell lysates) were transferred to fresh tubes. Concanavalin A Sepharose (Amersham/Pharmacia) beads were added to each sample (35 μ L of a 50% v/v slurry) and the samples were incubated at 4°C for 30 minutes. Concanavalin A Sepharose precipitates the cellular glycoproteins, which include ErbB family receptors. The precipitated glycoproteins were washed three times with 500 μ L ice-cold lysis buffer, then were eluted by boiling the beads for five minutes in 80 μ L reducing SDS protein sample buffer. The beads were collected by centrifugation and half of the eluted glycoproteins (40 μ L) were recovered and resolved by SDS/PAGE on a 7.5% acrylamide gel.

The resolved glycoproteins were electroblotted onto nitrocellulose (BiotraceNT – Gelman Sciences). The resulting blot was blocked by incubation for 45 minutes at room temperature in a solution consisting of 5% bovine serum albumin (Sigma) dissolved in Tris-buffered normal saline (TBS) supplemented with 0.05% Tween-20 (TBS-T). The blot was then probed with a mouse monoclonal antiphosphotyrosine antibody (4G10 – Upstate Biotechnology). The blot was washed with TBS-T 5

times for 6 minutes each, and primary antibody binding was detected by probing the blot with a goat anti-mouse antibody conjugated to horseradish peroxidase (HRP – Pierce). The blot was washed with TBS-T 12 times for 10 minutes each, after which HRP activity was visualized by enhanced chemiluminescence (ECL – Amersham Pharmacia Biotech). The resulting chemilumigrams were digitized using a Linotype-Hell Jade flatbed scanner and the amount of receptor tyrosine phosphorylation was quantified using NIH Image software. The amount of receptor tyrosine phosphorylation in samples from cells treated with a putative receptor tyrosine kinase inhibitor were compared to a standard curve generated using samples from cells treated with DMSO solvent control. This enabled us to determine the concentration of a given tyrosine kinase inhibitor that was necessary to cause a 50% reduction in receptor tyrosine phosphorylation. This value is reported as the receptor tyrosine phosphorylation IC₅₀ value.

Inhibition of Cellular DNA Synthesis. The assay for inhibition of cellular DNA synthesis was adapted from a previously-described protocol.⁵⁴ Briefly, human mammary (tumor) cells were seeded in 1 mL aliquots into 24-well culture dishes at a density of 10⁵ cells/well. Cells were incubated for 24 hours at 37°C, and a tyrosine kinase inhibitor dissolved in DMSO was added to each well in a volume of 10 µL. Each tyrosine kinase inhibitor was assayed at 3-5 different concentrations and each concentration was assayed using 3-4 wells of cells. Cells treated with 10 µl DMSO served as the solvent control. Cells were then incubated for 48 hours at 37°C. ³H-Thymidine (1.5 µCi – Amersham Pharmacia Biotech) dissolved in a 1.5 µL of an aqueous solution was added to each well and the cells were incubated for an additional 2 hours at 37°C. The culture medium was aspirated from the wells, and the cells were rinsed once with 1 mL ice-cold phosphate-buffered saline (PBS) and once with 1 mL ice-cold 10% trichloroacetic acid (TCA). Incorporated ³H-Thymidine was precipitated by incubating the cells for at least 30 minutes at 4°C in 1 mL 10% TCA. Following incubation, the TCA solution was aspirated from

each well and the precipitated (incorporated) ^3H -Thymidine was solubilized by incubating the cells for 30 minutes at 95°C in $500\ \mu\text{L}$ 3% perchloric acid. The perchloric acid extracts were transferred to scintillation vials containing 10 mL Cytosint scintillation cocktail (ICN). The incorporated ^3H -Thymidine was assayed by scintillation counting on a Packard Tricarb scintillation counter. The amount of ^3H -Thymidine incorporation observed in the cells treated with the solvent control was divided by 2 (two) to determine the amount of 1/2 maximal ^3H -Thymidine incorporation. Dose response curves for each combination of putative tyrosine kinase inhibitor and cell line were then constructed using the ^3H -Thymidine incorporation data. The dose response curves and the 1/2 maximal ^3H -Thymidine values were used to calculate the concentration of each inhibitor required to inhibit ^3H -Thymidine incorporation by 50% in a given cell line. This value is reported as the DNA synthesis IC_{50} value.

***In Vitro* EGFR Binding Assay.** EGFR tyrosine kinase receptor binding was determined by a competitive radiometric assay using [^{125}I]-4-(3'- [^{125}I]iodoanilino)-6,7-dimethoxyquinazoline³⁶ as the radiotracer (Specific Activity = 590 Ci/mmol). Various concentrations (10^{-11}M – 10^{-6}M) of the quinazoline compounds were prepared in binding buffer (10 mM HEPES, 1mM EDTA, 5 mM MgCl_2 , 0.1%BSA, 10 $\mu\text{g}/\text{mL}$ leupeptin, 10 $\mu\text{g}/\text{mL}$ pepstatin, 0.5 $\mu\text{g}/\text{mL}$ aprotin and 200 $\mu\text{g}/\text{mL}$ bacitracin (pH 7.4)). Commercially available (Receptor Biology, Beltsville, MD) A431 human carcinoma cell membrane were diluted in ice cold binding buffer (50 μL of 0.06 $\mu\text{g}/\mu\text{L}$ stock solution) and homogenized with a hand held homogenizer. This preparation was added to the buffer solution followed by the addition of 1 μCi of the radiotracer to initiate the binding assay. The mixture was incubated at room temperature in the dark for 60 min. The incubation was terminated by the addition of 5 mL of ice cold buffer (10 mM HEPES, 1 mM EDTA, 5 mM MgCl_2 , and 0.1% BSA (pH 7.4)) and the solutions were filtered through polyethylenamine soaked (0.5% soln., 30 min) GF/B filter paper (Brandel, Gaithersburg, MD) using a Brandel Cell Harvester, followed by two washes (5 mL each) with wash buffer. The filter paper was dried and counted for 10 minutes using a TM Analytic gamma well counter.

Non-specific binding was determined by adding 1 μ M 4-(3'-bromoanilino)-dimethoxy quinazoline to the assay. Inhibition constants at 50% of specific binding (IC_{50}) were derived from specific binding versus concentration curves. Triplicate assays were performed for each compound.

Acknowledgments

This work was supported in part by the Director, Office of Science, Office of Biological and Environmental Research, Medical Science Division of the U.S. Department of Energy under contract No. DE-AC03-76SF00098, the Army Medical Research and Materiel Command, U.S. Department of Defense under grant no. DAMD17-98-1-8064 (HFV) and grant no. DAMD17-00-1-0415 (DJR), NIH National Cancer Institute under grant no. R21CA79823 (HFV), R01CA094253 (HFV) and R21CA80770 (DJR) and the California Breast Cancer Research Program under grant no. 4IB-0059 (HFV). Support for Dr. John Lim was provided by NIH National Cancer Institute training grant no. T32CA66527 through the UCSF Department of Radiology (Randall Hawkins, M.D., Ph.D., P.I.). The authors wish to thank Dr. Scott Taylor for his helpful discussion and input on the radiometric binding assay. The authors also wish to thank Stephen Hanrahan for the preparation of the iodine-125 labeled quinazolines for the radiometric binding assay.

References

- (1) Hanks, S. K.; Quinn, A. M.; Hunter, T. The protein tyrosine kinase family: Conserved features and phylogeny of the catalytic domains. *Science* **1988**, *241*, 42-52.
- (2) Ullrich, A.; Schlessinger, J. Signal transduction by receptors with tyrosine kinase activity. *Cell* **1990**, *61*, 203-212.
- (3) Yarden, Y.; Ullrich, A. Growth Factor receptor tyrosine kinases. *Ann. Rev. Biochem.* **1988**, *57*, 443-478.
- (4) Downward, J.; Yarden, Y.; Mayes, E.; Scrace, G.; Totty, N. et al. Close similarity of epidermal growth factor receptor and v-erb-B oncogene protein sequences. *Nature* **1984**, *307*, 521-527.
- (5) Ullrich, A.; Coussens, L.; Hayflick, J. S.; Dull, T. J.; Gray, A. et al. Human epidermal growth factor receptor cDNA sequence and aberrant expression of the amplified gene in A431 epidermoid carcinoma cells. *Nature* **1984**, *309*, 418-425.
- (6) Yarden, Y. The EGFR family and its ligands in human cancer: signalling mechanisms and the therapeutic opportunities. *Eu. J. Cancer* **2001**, *37*, S3-S8.
- (7) Yarden, Y.; Sliwkowski, M. X. Untangling the ErbB signalling network. *Nat. Rev. Mol. Cell Biol.* **2001**, *2*, 127-137.
- (8) Gasparini, G.; Bevilacqua, P.; Pozza, F.; Meli, S.; Boracchi, P. et al. Value of epidermal growth factor receptor status compared with growth fraction and other factors for prognosis in early breast cancer. *Br. J. Cancer* **1992**, *66*, 970-976.
- (9) Toi, M.; Nakamura, T.; Mukaida, H.; Wada, T.; Osaki, A. et al. Relationship between epidermal growth factor receptor status and various prognostic factors in human breast cancer. *Cancer* **1990**, *65*, 1980-1984.
- (10) Klijn, J.; Berns, P.; Schmitz, P.; Foekens, J. The clinical significance of epidermal growth factor receptor (EGF-R) in human breast cancer: A review on 5232 patients. *Endocrine Rev.* **1992**, *13*, 3-17.

- (11) Koenders, P.; Beex, L.; Geurts-Moespot, A.; Heuvel, J.; Kienhuis, C. et al. Epidermal growth factor receptor-negative tumors are predominantly confined to the subgroup of estradiol receptor-positive human primary breast cancers. *Cancer Res.* **1991**, *51*, 4544-4548.
- (12) Mori, T.; Morimoto, T.; Komaki, K.; Monden, Y. Comparison of estrogen receptor and epidermal growth factor receptor content of primary and involved nodes in human breast cancer. *Cancer* **1991**, *68*, 532-537.
- (13) Bridges, A. J. The rationale and strategy used to develop a series of highly potent, irreversible, inhibitors of the epidermal growth factor receptor family of tyrosine kinases. *Curr. Med. Chem.* **1999**, *6*, 825-843.
- (14) Levitzki, A. Protein tyrosine kinase inhibitors as novel therapeutic agents. *Pharmacol. Ther.* **1999**, *82*, 231-239.
- (15) Shawver, L. K.; Slamon, D.; Ullrich, A. Smart drugs: tyrosine kinase inhibitors in cancer therapy. *Cancer Cell* **2002**, *1*, 117-123.
- (16) Traxler, P.; Furet, P. Strategies toward the design of novel and selective protein tyrosine kinase inhibitors. *Pharmac. Ther.* **1999**, *82*, 195-206.
- (17) Woodburn, J. R. The epidermal growth factor receptor and its inhibition in cancer therapy. *Pharmac. Ther.* **1999**, *82*, 241-250.
- (18) Mendelsohn, J.; Baselga, J. The EGF receptor family as targets for cancer therapy. *Oncogene* **2000**, *19*, 6550-6565.
- (19) Carpenter, G. Receptors for epidermal growth factor and other polypeptide mitogens. *Ann. Rev. Biochem.* **1987**, *56*, 881-914.
- (20) Andersson, A.; Capala, J.; Carlsson, J. Effects of EGF-dextran-tyrosine-131I conjugates on the clonogenic survival of cultured glioma cells. *J. Neurooncol.* **1992**, *14*, 213-223.
- (21) Schatten, C.; Patiesky, N.; Vavra, N.; Ehrenbock, P.; Angelberger, P. et al. Lymphoscintigraphy with 123I-labeled epidermal growth factor. *Lancet* **1991**, *337*, 395-396.

- (22) Orlova, A.; Bruskin, A.; Sjostrom, A.; Lundqvist, H.; Gedda, L. et al. Cellular Processing of ¹²⁵I- and ¹¹¹In-labeled epidermal growth factor (EGF) bound to cultured A431 tumor cells. *Nuc. Med. Biol.* **2000**, *27*, 827-835.
- (23) Capala, J.; Barth, R. F.; Bailey, M. Q.; Fenstermaker, R. A.; Marek, M. J. et al. Radiolabeling of epidermal growth factor with ^{99m}Tc and in vivo localization following intracerebral injection into normal and glioma-bearing rats. *Bioconj. Chem.* **1997**, *8*, 289-295.
- (24) Rusckowski, M.; Qu, T.; Chang, F.; Hnatowich, D. J. Technetium-^{99m} labeled epidermal growth factor-tumor imaging in mice. *J. Peptide Res.* **1997**, *50*, 393-401.
- (25) Yang, W.; Barth, R. F.; Leveille, R.; Adams, D. M.; Ciesielski, M. et al. Evaluation of systemically administered radiolabeled epidermal growth factor as a brain tumor targeting agent. *J. Neurooncol.* **2001**, *55*, 19-28.
- (26) Reilly, R. M.; Kiarash, R.; Cameron, R. G.; Porlier, N.; Sandhu, J. et al. ¹¹¹In-labeled EGF is selectively radiotoxic to human breast cancer cells overexpressing EGFR. *J. Nucl. Med.* **2000**, *41*, 429-438.
- (27) Remy, S.; Reilly, R.; Sheldon, K.; Garipey, J. A new radioligand for the epidermal growth factor receptor: ¹¹¹In labeled human epidermal growth factor derivitized with a bifunctional metal-chelating peptide. *Bioconj. Chem.* **1995**, *6*, 683-690.
- (28) Reilly, R. M.; Kiarash, R.; Sandhu, J.; Lee, Y. W.; Cameron, R. G. et al. A comparison of EGF and MAb 528 labeled with ¹¹¹In for imaging human breast cancer. *J. Nucl. Med.* **2000**, *41*, 903-911.
- (29) Cammilleri, S.; Kaphan, G.; Berthois, Y.; Siles, S.; Khelifa, F. et al. Biodistribution and imaging studies with radioactively labeled monoclonal antibody anti-epidermal growth factor receptor in athymic mice bearing human mammary tumor. *Antibody Immunoconjugates Radiopharm.* **1991**, *4*, 501-506.
- (30) Kalofonos, H.; Pawlikowska, T.; Hemingway, A.; Courtenay-Luck, N.; Dhokia, B. et al. Antibody guided diagnosis and therapy of brain gliomas using radiolabeled monoclonal

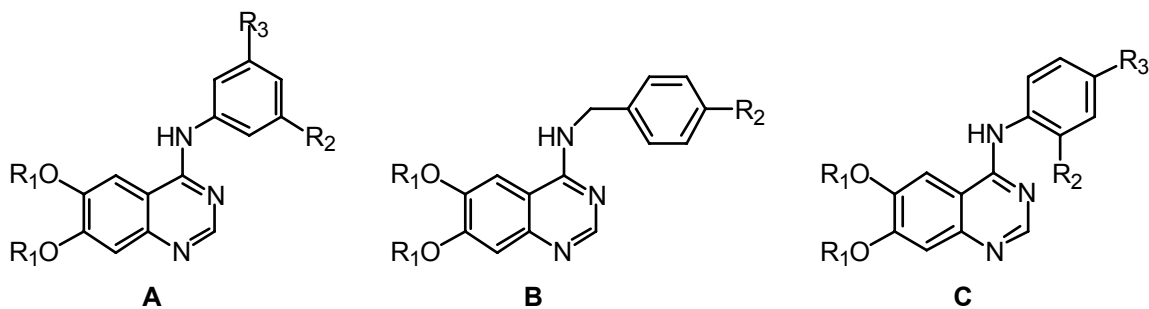
antibodies against epidermal growth factor receptor and placental alkaline phosphatase. *J. Nucl. Med.* **1989**, *20*, 1636-1645.

- (31) Divgi, C. R.; Welt, S.; Kris, M.; Real, F. X.; Yeh, S. D. et al. Phase I and imaging trial of indium 111-labeled anti-epidermal growth factor receptor monoclonal antibody 225 in patients with squamous cell lung carcinoma [see comments]. *J. Natl. Cancer Inst.* **1991**, *83*, 97-104.
- (32) Ramos-Suzarte, M.; Rodriguez, N.; Oliva, J. P.; Iznaga-Escobar, N.; Perera, A. et al. 99mTc-labeled antihuman epidermal growth factor receptor antibody in patients with tumors of epithelial origin: Part III. Clinical trials safety and diagnostic efficacy. *J. Nucl. Med.* **1999**, *40*, 768-775.
- (33) Bridges, A. J.; Zhou, H.; Cody, D. R.; Rewcastle, G. W.; McMichael, A. et al. Tyrosine kinase inhibitors. 8. An unusually steep structure-activity relationship for analogues of 4-(3-bromoanilino)-6,7-dimethoxyquinazoline (PD 153035), a potent inhibitor of the epidermal growth factor receptor. *J. Med. Chem.* **1996**, *39*, 267-276.
- (34) Fry, D.; Kraker, A.; McMichael, A.; Ambroso, L.; Nelson, J. et al. A specific inhibitor of the epidermal growth factor receptor tyrosine kinase. *Science* **1994**, *265*, 1093-1095.
- (35) Rewcastle, G.; Denny, W.; Bridges, A.; Zhou, H.; Cody, D. et al. Tyrosine kinase inhibitors. 5. Synthesis and structure-activity relationships for 4-[(phenylmethyl)amino]- and 4-(phenylamino)quinazolines as potent adenosine 5'-triphosphate binding site inhibitors of the tyrosine kinase domain of the epidermal growth factor receptor. *J. Med. Chem.* **1995**, *38*, 3482-3487.
- (36) Lim, J. K.; Negash, K.; Hanrahan, S. M.; VanBrocklin, H. F. Synthesis of 4-(3'-[¹²⁵I]iodoanilino)-6,7-dialkoxyquinazolines: Radiolabeled epidermal growth factor tyrosine kinase inhibitors. *J. Lab. Compd. Radiopharm.* **2000**, *43*, 1183-1191.
- (37) Mulholland, G. K.; Winkle, W.; Moch, B. H.; Sledge, G. Radioiodinated Epidermal Growth Factor Receptor Ligands as tumor probe. Dramatic potentiation of binding to MDA-486 cancer cells in presence of EGF. *J. Nucl. Med.* **1995**, *36*, 71P.

- (38) Bonasera, T. A.; Ortu, G.; Rozen, Y.; Kraus, R.; Freedman, N. M. et al. Potential (18)F-labeled biomarkers for epidermal growth factor receptor tyrosine kinase. *Nucl. Med. Biol.* **2001**, *28*, 359-374.
- (39) Snyder, S. E.; Sherman, P. S.; Blair, J. B. 4-(3-chloro-4-[18F]fluorophenylamino)-6,7-dimethoxyquinazoline: A radiolabeled EGF receptor inhibitor for imaging tumor biochemistry with PET. *J. Nucl. Med.* **2000**, *41 Suppl.*, 233p.
- (40) Mulholland, G. K.; Zheng, Q.-H.; Winkle, W. L.; Carlson, K. A. Synthesis and Biodistribution of new C-11 and F-18 labeled epidermal growth factor receptor ligands. *J. Nucl. Med.* **1997**, *38*, 141P.
- (41) Johnstrom, P.; Fredriksson, A.; Thorell, J.-O.; Stone-Elander, S. Synthesis of [Methoxy-11C]PD153035, a selective EGF receptor Tyrosine Kinase Inhibitor. *J. Lab. Compd. Radiopharm.* **1998**, *41*, 623-629.
- (42) Fredriksson, A.; Johnstrom, P.; Thorell, J.-O.; von Heijne, G.; Hassan, M. et al. In vivo evaluation of the biodistribution of 11C-labeled PD153035 in rats without and with neuroblastoma implants. *Life Sci.* **1999**, *65*, 165-174.
- (43) Johnstrom, P.; Fredriksson, A.; Thorell, J.-O.; Hassan, M.; Kogner, P. et al. Synthesis and in vivo biodistribution of tyrosine kinase inhibitor, [Methoxy-11C]PD 153035. *J. Lab. Compd. Radiopharm.* **1997**, *40*, 377-379.
- (44) Minick, D.; Frenz, J.; Patrick, M.; Brent, D. A comprehensive method for determining hydrophobicity constants by reversed-phase high-performance liquid chromatography. *J. Med. Chem.* **1988**, *31*, 1923-1933.
- (45) Pomper, M.; VanBrocklin, H.; Thieme, A.; Thomas, R.; Kiesewetter, D. et al. 11 β -methoxy-, 11 β -ethyl- and 17 α -ethynyl-substituted 16 α -fluoroestradiols: receptor-based imaging agents with enhanced uptake efficiency and selectivity. *J. Med. Chem.* **1990**, *33*, 3143-3155.
- (46) Eckelman, W. The application of receptor theory to receptor-binding and enzyme-binding oncologic radiopharmaceuticals. *Nucl. Med. Biol.* **1994**, *21*, 759-769.
- (47) Eckelman, W. C. Sensitivity of New Radiopharmaceuticals. *Nucl. Med. Biol.* **1998**, *25*, 169-173.

- (48) Kuhnast, B.; Dolle, F.; Vaufrey, F.; Hinnen, F.; Crouzel, C. et al. Fluorine-18 labeling of oligonucleotides bearing chemically-modified ribose-phosphate backbones. *J. Lab. Compd. Radiopharm.* **2000**, *V43*, 837-848.
- (49) Mishani, E.; Cristel, M. E.; Dence, C. S.; McCarthy, T. J.; Welch, M. J. Application of a novel phenylpiperazine formation reaction to the radiosynthesis of a model fluorine-18-labeled radiopharmaceutical (18FTFMPP). *Nucl. Med. Biol.* **1997**, *24*, 269-273.
- (50) Mu, F.; Coffing, S. L.; Riese, D. J. I.; Geahlen, R. L.; Verdier-Pinard, P. et al. Design, synthesis, and biological evaluation of a series of lavendustin A analogues that inhibit EGFR and Syk tyrosine kinases, as well as tubulin polymerization. *J. Med. Chem.* **2001**, *44*, 441-452.
- (51) Plowman, G. D.; Green, J. M.; Culouscou, J. M.; Carlton, G. W.; Rothwell, V. M. et al. Heregulin induces tyrosine phosphorylation of HER4/p180erbB4. *Nature* **1993**, *366*, 473-475.
- (52) Riese, D. J. I.; Komurasaki, T.; Plowman, G. D.; Stern, D. F. Activation of ErbB4 by the bifunctional epidermal growth factor family hormone epiregulin is regulated by ErbB2. *J. Biol. Chem.* **1998**, *273*, 11288-11294.
- (53) Riese, D. J., 2nd; van Raaij, T. M.; Plowman, G. D.; Andrews, G. C.; Stern, D. F. The cellular response to neuregulins is governed by complex interactions of the erbB receptor family. [Erratum In: *Mol Cell Biol* 1996 Feb;16(2):735]. *Mol. Cell. Biol.* **1995**, *15*, 5770-5776.
- (54) Hwang, E. S.; Riese, D. J. I.; Settleman, J.; Nilson, L. A.; Honig, J. et al. Inhibition of cervical carcinoma cell line proliferation by the introduction of a bovine papillomavirus regulatory gene. *J. Virol.* **1993**, *67*, 3720-3729.
- (55) Gazit, A.; Oshero, N.; Gilon, C.; Levitzki, A. Tyrphostins. 6. Dimeric benzylidenemalononitrile tyrophostins: potent inhibitors of EGF receptor tyrosine kinase in vitro. *J. Med. Chem.* **1996**, *39*, 4905-4911.
- (56) Dischino, D.D.; Welch, M.J.; Kilbourn, M.R.; Raichle, M.E. Relationship between lipophilicity and brain extraction of C-11 labeled radiopharmaceuticals. *J. Nucl. Med.* **1983**, *24*, 1030-1038.

- (57) **Katzenellenbogen, J.A.; Heiman, D.F.; Carlson, K.E.; Lloyd, J.E.** In vivo and in vitro steroid receptor assays in the design of estrogen radiopharmaceuticals. In Eckelman, W.C. *Receptor-Binding Radiotracers*; CRC Press: Boca Raton, **1982**; Volume I, Chapter 6; pp 93-126.
- (58) Srinivasan, R., Poulosom, R., Hurst, H.C. and Gullick, W.J. Expression of the c-erbB-4/HER4 protein and mRNA in normal human fetal and adult tissues and in a survey of nine solid tumour types. *J. Pathol.* **1998**, *185*, 236-245.
- (59) Bacus, S.S., Chin, D., Yarden, Y., Zelnick, C.R. and Stern, D.F. Type 1 receptor tyrosine kinases are differentially phosphorylated in mammary carcinoma and differentially associated with steroid receptors. *Am. J. Pathol.* **1996**, *148*, 549-558.

Table 1. 4-Anilino- and 4-Benzylamino- Quinazolines Chemical and Physical Data.

no.	type	R ₁	R ₂	R ₃	mp (°C)	formula	anal.	Log P _{o/w} ^a
10a	A	CH ₃ CH ₂	F	H	247-248	C ₁₈ H ₁₈ FN ₃ O ₂ •HCl	C, H, N	3.71 ± 0.12
10b	A	CH ₃ CH ₂	Cl	H	260-261	C ₁₈ H ₁₈ ClN ₃ O ₂ •HCl	C, H, N	4.31 ± 0.26
10c	A	CH ₃ CH ₂	Br	H	250-252	C ₁₈ H ₁₈ BrN ₃ O ₂	C, H, N	4.40 ± 0.25
10d	A	CH ₃ CH ₂	I	H	258-261	C ₁₈ H ₁₈ IN ₃ O ₂ •HCl	C, H, N	4.62 ± 0.26
11a	A	CH ₃	F	H	244.5-246	C ₁₆ H ₁₄ FN ₃ O ₂ •1.1HCl	C, H, N	2.96 ± 0.10
11b	A	CH ₃	Cl	H	230-235	C ₁₆ H ₁₄ ClN ₃ O ₂ •HCl	C, H, N	3.51 ± 0.23
11c	A	CH ₃	Br	H	256-257.5	C ₁₆ H ₁₄ BrN ₃ O ₂ •HCl	C, H, N	3.49 ± 0.22
11d	A	CH ₃	I	H	251-251.5	C ₁₆ H ₁₄ IN ₃ O ₂ •HCl	C, H, N	3.65 ± 0.22
12	A	CH ₃ CH ₂	F	CF ₃	278-280	C ₁₉ H ₁₇ F ₄ N ₃ O ₂ •HCl	C, H, N	5.49 ± 0.29
13	A	CH ₃	F	CF ₃	269-270.5	C ₁₇ H ₁₃ F ₄ N ₃ O ₂ •HCl	C, H, N	4.66 ± 0.26
14	B	CH ₃ CH ₂	F	-	238.5-240	C ₁₉ H ₂₀ FN ₃ O ₂	C, H, N	3.78 ± 0.23
15	B	CH ₃	F	-	250-251	C ₁₇ H ₁₆ FN ₃ O ₂ •HCl	C, H, N	3.02 ± 0.20
16a	C	CH ₃ CH ₂	F	H	252-255	C ₁₈ H ₁₈ FN ₃ O ₂ •1.4HCl	C, H, N	3.02 ± 0.11
16b	C	CH ₃ CH ₂	H	F	220.5-222	C ₁₈ H ₁₈ FN ₃ O ₂ •HCl	C, H, N	3.73 ± 0.23
17a	C	CH ₃	F	H	247-248	C ₁₆ H ₁₄ FN ₃ O ₂ •HCl	C, H, N	2.20 ± 0.11
17b	C	CH ₃	H	F	231-232	C ₁₆ H ₁₄ FN ₃ O ₂ •HCl	C, H, N	2.87 ± 0.21

^a Estimated by the reversed-phase HPLC method of Minick, et al.⁴⁴

Table 2. Biochemical data for the EGFR tyrosine kinase (tk) inhibitors

no.	Receptor Binding	Receptor Phosphorylation		
	(IC ₅₀ nM)	(IC ₅₀ nM)		
	EGFR tk	EGFR tk	ErbB2 tk	ErbB4 tk
10a	8.17 ± 1.57	6.5 ± 2.1		
10b	0.38 ± 0.13	1.2 ± 0.2		
10c	0.41 ± 0.09	3.2 ± 0.8	215 ± 87	50 ± 19
10d	0.64 ± 0.15	4.6 ± 2.0	69 ± 10	59 ± 29
11a	31.9 ± 7.00	6.3 ± 2.0		
11b	1.26 ± 0.00	0.8 ± 0.2		
11c	0.66 ± 0.12	2.6 ± 0.5	143 ± 52	49 ± 16
11d	1.05 ± 0.51	6.4 ± 2.7		
12	8.95 ± 3.26	>50		
13	20.0 ± 10.2	19.1 ± 2.9		
14	17.0 ± 5.0	6.6 ± 1.6	231 ± 92	>100
15	47.7 ± 14.1	10.9 ± 2.8		
16a	9.31 ± 1.19	15.8 ± 2.2		
16b	16.0 ± 3.7	23.1 ± 4.2		
17a	32.2 ± 7.4	12.8 ± 3.5		
17b	51.0 ± 11.7	19.1 ± 2.5		

Table 3. Inhibition of DNA Synthesis (IC₅₀ nM)

no.	MCF-10A ^a	MCF-7 ^b	MCF-7/ MCF-10A
10a	99 ± 16	1923 ± 456	19.5
10b	108 ± 8	1087 ± 402	10.1
10c	78 ± 12	1695 ± 169	21.7
10d	153 ± 25	1571 ± 263	10.3
11a	59 ± 5	1956 ± 842	33.2
11b	173 ± 24	1982 ± 387	11.5
11c	211 ± 45	1613 ± 123	7.6
11d	585 ± 108	2433 ± 61	4.2
12	>3000	N.D.	--
13	1634 ± 100	4717 ± 1014	2.9
14	188 ± 25	1433 ± 88	7.6
15	489 ± 87	>7000	
16a	141 ± 17	1101 ± 656	7.8
16b	622 ± 69	7487 ± 505	12.0

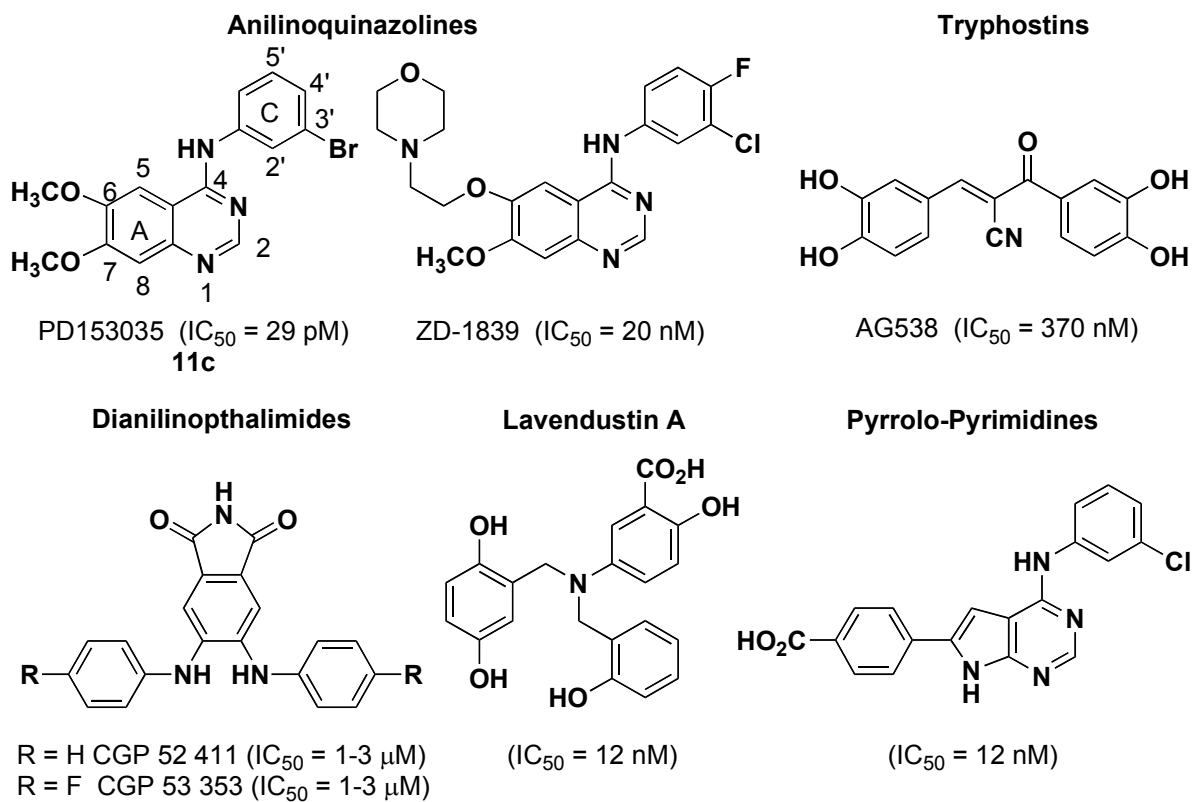
17a	179 ± 31	1950 ± 260	10.9
17b	612 ± 134	3375 ± 686	5.5

^a EGF-dependent human mammary epithelial cell line
^b EGF-independent human mammary tumor cell line

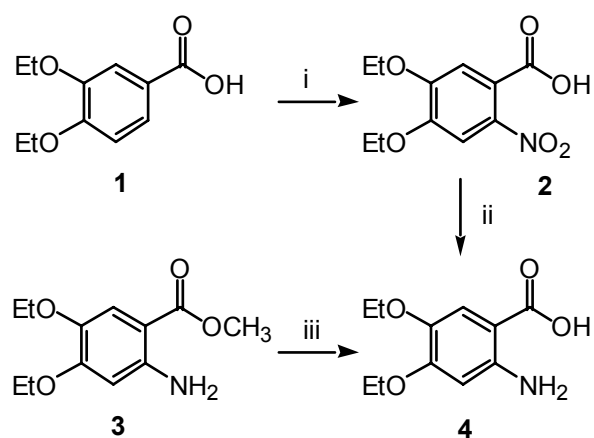
Figure Captions:

Figure 1. EGFR tyrosine kinase inhibitors^{13,16,34,55}

Figure 1.

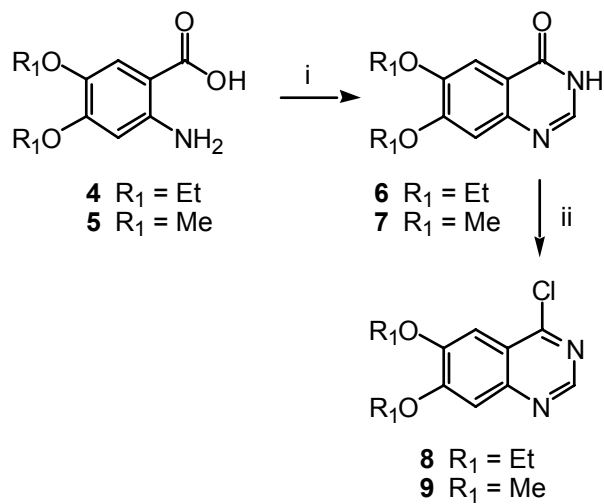


Scheme 1



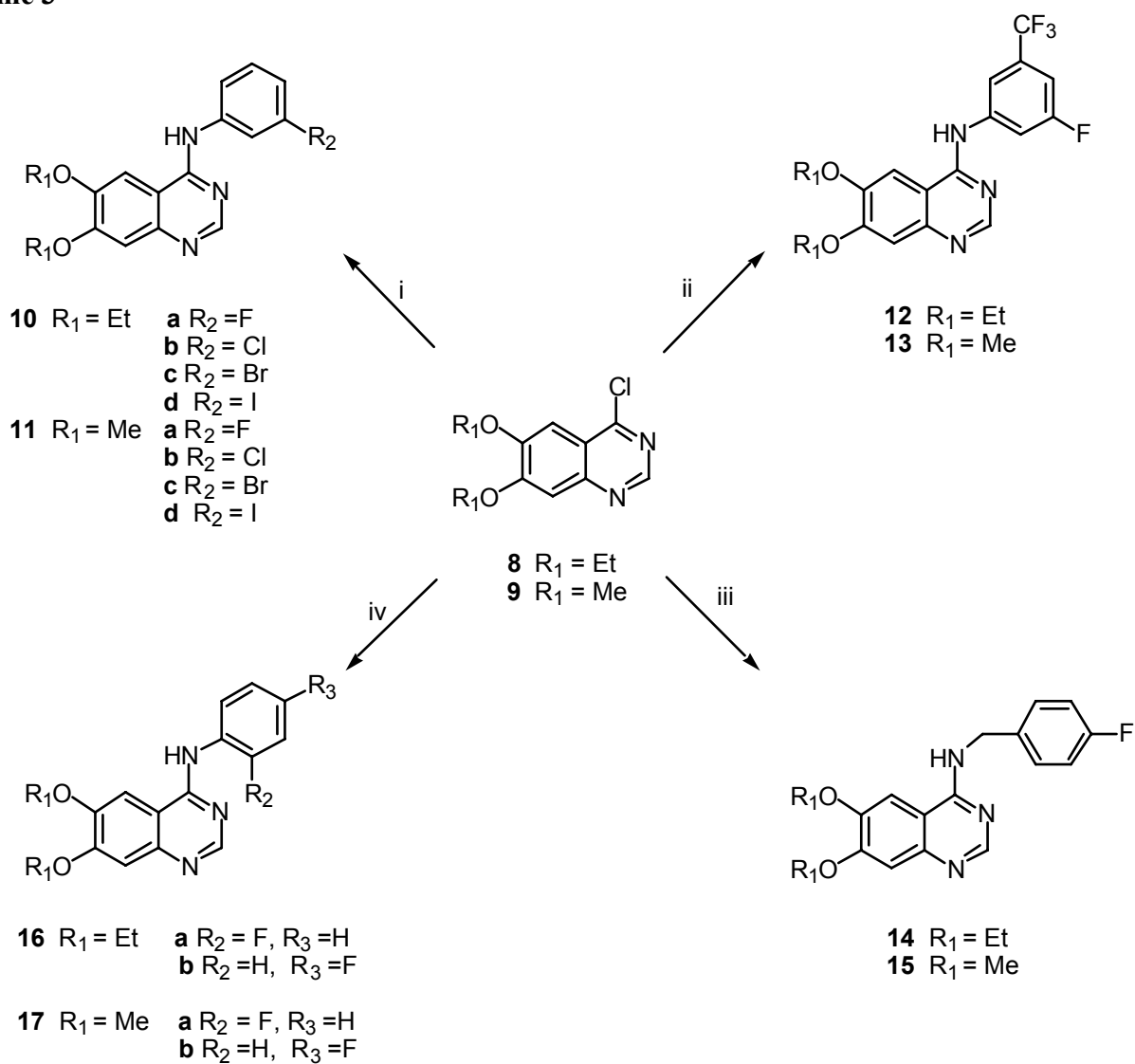
(i) 70% HNO_3 / glacial acetic acid/ 2 h/ RT;
 (ii) SnCl_2 / HCl / 2 h/ RT; (iii) NaOH /
 reflux/1 h, then HCl

Scheme 2



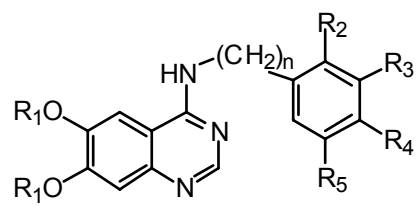
(i) formamidine•HCl/ heat then NaOH/
sonicate/ 1 h/ RT; (ii) oxalyl chloride/ DMF/
1,2-dichloroethane/ reflux

Scheme 3



(i) 3-haloaniline/ DMF/ heat; (ii) 3-fluoro-5-trifluoromethylaniline/ DMF/ heat;
 (iii) 4-fluorobenzylamine/ DMF/ heat.; (iv) 2- or 4-fluoroaniline/ DMF/ Heat

Table of Contents graphic



$R_1 = \text{Me or Et}$
 $n = 0 \text{ or } 1$